A Study on Inelastic Behaviors of 3-D Steel Frames Considering the Effect of Varying Axial Loads on Columns

by Yiyi CHEN(I), Ken-ichi OHI(II), Koichi TAKANASHI(III)

1. Introduction

A considerable amount of axial load change will occur in the side or corner columns at lower stories of high-rise or middle-rise buildings due to overturning. Usually axial loads on columns are regarded as constant and equal to the initial gravity loads for simplicity in design. Thus two changes resulted from varying axial load are often omitted in the design process, one of which is the change of moment capacity of columns, and the other is the difference of compressive deformation of columns.

The effects of such a varying axial loads on steel beam-columns in planer frames have been experimentally studied by the authors[1]. A simple steel beam-column analysis model that can describe the behaviors with sufficient accuracy has also been developed[2]. In this paper, the model is expanded so that the behaviors of beam-columns in three-dimensional(3-D) frames can be simulated. An experimental study on steel beam-columns subjected to varying axial loads and bi-directional horizontal loads is carried out, and the validity of the analysis model is checked. Finally, a simple frame model is numerically analyzed to investigate the effects of varying axial loads on 3-D steel frames.

2. Analysis Models of Steel Beam-column

A steel beam-column is regarded as an assembly of two kinds of elements as shown in Fig.1: one is an elastic beam, and the other is an inelastic joint. In the analysis, nodes are located at the tips of these elements. Geometrical non-linearity or P-Δ effect is considered only for the nodal displacements by updating each element coordinate system in the incremental analysis.

Each inelastic joint consists of several axial springs, two elastic shear panels, and one elastic torsional spring, as shown in Fig.2. The axial springs are located on the central lines of flanges or webs, and the area and location of each spring are so arranged that the section area and plastic section modulus are the same as those of the original section. Fig.3 gives an example that shows how the relation of axial load and moment capacities of multi-spring joint with only 8 axial springs is similar to box sectional column.

The skeleton curve to describe the behavior of each axial spring is arranged as a piecewise linear model as shown in Fig.4(a). Two imaginary points termed 'target point' on the skeleton curves, one at each side, are considered herein. Each target point is set to the elastic-limit point in the initial state. When a loading beyond the elastic-limit is made along one side of the skeleton with a certain amount of plastic displacement increment, the target point of the loading side moves together with the loading point. At the same time, the other side of skeleton curve including the other target point shall be shifted to the loading direction as much as ψ times the plastic displacement increment as shown in Fig.4(b). If ψ is set to zero, neither hardening nor degrading occurs during reversals within the past peak amplitudes. If ψ is set to one, the hysteresis includes no softening due to the Bauschinger effect. Actual behaviors of steel members are believed to fall into the intermediate state between these two extremes.

Unloading and reloading paths are modeled as portions of the Ramberg-Osgood function

(I)Research Associate, Institute of Industrial Science, Univ. of Tokyo (II)Associate Professor, Institute of Industrial Science, Univ. of Tokyo
(III)Professor, Institute of Industrial Science, Univ. of Tokyo

shown in the Fig.4(c). As for the hysteresis parameters, ψ and r, they can be selected referring to the results of uniaxial cyclic tests[3,4] as shown in Fig.5.

3. Experimental Study

To check the validity of the analysis model, a series of tests on beam–columns under varying axial loads and uni–directional or bi–directional lateral loads are carried out.

A fictitious structural system as shown in Fig 6.(b) is considered. A triangular–column rigid body is supported by a single column 1.5 meter long and two idealistic pin–roller supports. A vertical load denoted by 3Nc are applied to the geometrical center of the rigid body. Bi–directional horizontal loads denoted by Qx and Qy are applied on the column axis at the height of 15 meters from the column top. The column foot and the column top are rigidly connected to the basement and the rigid body, respectively. The vertical displacement at each pin–roller support is constrained to be the same as the vertical displacement at the column top, that is, it is assumed that neither pitching nor rolling of the rigid body occurs. From the equilibrium condition of the rigid body, the varying axial load denoted by N satisfies the following equation, where the secondary torsion effects due to the column top displacements are ignored:

$$N-Nc = 5.25(Qx+Qy) + N(Ux+Uy)/600 \qquad (1)$$

where, Ux,Uy: Horizontal displacements at the column top in centimeters

The 3–D structural system is easily simplified into 2–D structural system as shown in Fig.6(a), and Eq.(1) may also be used in this case if terms Qx and Ux are supposed to be zero.

In the test procedure, the resistance terms as well as the displacement terms in Eq.(1) are obtained from the loading test and used to determine the axial load change that shall be applied simultaneously to the specimen. The column in such a fictitious structural system is tested in the test rig as shown in Fig.7, where two identical specimens are connected to each other and loaded by two transverse jacks at the joint. One end of the specimens is completely fixed and the other is fixed to a roller support loaded by an axial jack. The specimens have the same box shape section being 120 mm in width and 9 mm in thickness.

Three kinds of loading tests are performed: (1) monotonic loading tests, (2) cyclic loading tests and (3) pseudo dynamic earthquake response tests. Fifty percent of the yield axial force is commonly assigned for the initial magnitude of the axial load, Nc, of each test case. The ratio of bi–directional load, Qy/Qx, is kept at $\sqrt{3}$ during both monotonic and cyclic tests on 3–D structural system. The displacement along the y–axis, Uy, is controlled according to a prepared loading program. The loading program contains two cyclic reversals for each displacement amplitude level.

In the pseudo–dynamic tests, fictitious mass as much as (2Nc/g) is placed on the specimen axis at the height of 15 meters from the column top. The natural periods along two principal directions of the system are about one second. The ground acceleration for y–axis is the N–S component recorded at El Centro in 1940, the peak acceleration of which is scaled to 70/cm/sec/sec. This intensity corresponds to about 5 times of the intensity that causes the elastic shear response equal to the nominal yield strength of the specimen. The E–W component of El Centro scaled proportionally to 42 cm/sec/sec is used for the x–axis ground motion. No fictitious damping is assumed in the pseudo–dynamic tests.

4. Results of Tests and Analysis by Multi–spring Model

The results of tests compared with the analysis of their simulation are shown from Fig.8 to Fig.12. Here, Ux and Uy refer to the lateral displacements of columns; Qx and Qy to the restor–

ing forces of columns; Q_{30} to the resultant resistance; U_{30} is the corresponding displacement in this direction; N is axial load applied on columns; Mx and My are end moments of columns about x-axis and y-axis, respectively. L is the length of the columns. Mp is full-plastic moment and Qp is defined equal to 2Mp/L. The 15cm long parts at both two ends of the specimen are substituted by an inelastic joint model in the analysis. The parameters of the joint are derived from material tests and the hysteresis parameters, ψ and r, are assumed to be 0.85 and 5, respectively.

Simulation of columns at push side agrees with the results of monotonic tests quite well(Fig.8 and 9), where 'push side' means that the compression in the specimen increases according as the lateral load increases while 'pull side' means that the compression in the specimen decreases while the lateral load increases. Though in the case of columns at pull side, some differences appear after yielding obviously because near the yield point the varying axial load on the columns is close to zero and the multi-spring model gives a conservative approximation to the moment capacity in this range (Fig.3(c)), the whole behaviors are well simulated by the analysis model.

In both cyclic tests, the plastic deformation along the x-axis (bent about the y-axis of the cross section) was cumulated so much to one side that the test was terminated. These phenomena can be explained schematically from the behavior of the stress point as well as the normality rule of the plastic strain rate in the theory of plasticity. Fig.13 shows schematic illustration of the projection of the stress point to the Mx-My plane in the case of 3-D system. When the positive and the negative amounts of plastic rotation, bent about the x-axis, are controlled to be almost the same, the difference between the positive and the negative amounts of plastic rotation bent about the y-axis will be greater and greater according as the trajectory of the stress point shifts. Finally when stress point enters the region of $Mx>0$ and $My<0$ from the region of $Mx>0$ and $My>0$, the sign of plastic deformation becomes opposite to the former state. The phenomenon in the 2-D case can be explained in the same way but here the moment out of the flexural plane occurs due to geometrical imperfection and eccentricity.

The hysteresis curves observed in pseudo-dynamic test are shown in Fig.12. Because of the difference between the push side and the pull side restoring forces, the plastic deformation occurs mainly during the push side loading. In two of the four main yield excursions along the y-axis, the recovering of the resistance is observed. Such a recovering is corresponding to the trajectory of the stress point in the region of $Mx\ My<0$. This condition means that the effects of the overturning in the two directions are canceled by each other, and that the axial load returns to its initial value.

The above-mentioned aspects of hysteresis behavior as well as the shape of the hysteresis loops and the maximum resistance, are well simulated by the present model and analysis. Especially in the cyclic loading cases, the simulated hysteresis loops to the final stage, including the unstable cumulation of the plastic deformation, agree with the test results fairly well.

5. Frame Analysis

A simple 3-D frame model with a stiff upper structure and 4 columns at the lowest story as shown in Fig.14 is used to investigate the effects of varying axial load of columns on the whole frame's behavior that can not be sufficiently demonstrated by the test fictitious structural model with only one column. The span, the length and the cross-section of columns, the magnitude of initial axial load on each column, and the natural periods along two principal axes of the frame, all of these are arranged in the same way as the test model. In the static load analysis, horizontal load is applied to the center of gravity that is supposed to be 15 meter in height from the column top, at an angle of 0 or 30 degrees to the Y-axis, one of the principal axes of the frame. In the earthquake response analysis a lumped mass is put at that point, too. To make a comparison, an extremely large span is given to another frame model so that almost no axial load change occurs

in the columns. Because in such a comparative frame model, there is neither difference of moment capacity between columns and nor declination of the upper part of the structure, the behaviors of the model can be represented by one of its columns. This column is to be compared with the frame considering varying axial loads.

Fig. 15 shows the resistance vs. lateral displacement of columns in case that a monotonic horizontal load is applied along the Y-axis of the frame. Resistance of columns at push side here is lower than that in test model (see Fig.8(b)). The reason is as follows. In the analyzed frame model there are columns on both push and pull sides while only one column exists in the test model. Therefore, the total resistance and the amplitude of axial load change that is nearly proportional to the total resistance are larger in the analyzed frame model. The larger the compressive axial load of column is, the lower the resistance of the column becomes. By the same reason, the axial load on columns at pull side of the analyzed model decreases much less than that in the test model at the point of yield. As a result, the hardening effect of moment after yield becomes lower; the influence of P-Δ effect appears obviously; the resistance downs at once after yield. Though the resistance of column at push side is much lower, the average resistance of push side and pull side, or, in other words, the total resistance of the frame, is only a little lower than that under constant axial load.

However, when horizontal load is applied at 30 degrees to one of the principal axes, the average or the total resistance is about 18 percent lower than that under constant axial load (Fig.16(c)). Compared with the former case in which horizontal load is applied in one principal axis, the arm of the overturning moment becomes longer, but the columns at the both remotest sides from the center are less than those in the former case. Consequently, the amplitude of axial load change on corner column becomes larger than that in the former case. Thus the resistance of the column at the push side becomes less than that in the former case, and the increase of the resistance at the pull side can not make up for the loss at the push side. On such a condition if the effect of varying axial loads is not under consideration, the resistance of the frame will be overestimated.

The same motion as used in the test is also adopted in the frame response analysis, but its intensity is scaled to two times of the test value. The Y-axis is corresponding to the N-S component recorded at El Centro in 1940, and X-axis to the E-W component. Figs.17(a) through (d) show the hysteresis loops, base shear vs. the displacement at the central point on the top floor, of the frame model and the model under constant axial load. The dot curves in these figures are the results under static load applied in the direction of one principal axis. Fig.17(c) and (d) show the locus of displacements and base shears, respectively. In the case of varying axial load, the frame becomes more flexible, because the upper portion of the frame declines due to the different compressive deformations of columns. The maximum displacements along the Y-axis are almost the same, but along the X-axis the maximum displacement of frame model is larger when the influence of varying axial loads is considered. The restoring force is lower than that under constant axial load, which is the same phenomenon as observed in static analysis.

6. Concluding Remarks

A simplified constitutive modeling is developed for inelastic portions of steel beam-columns, by which the inelastic behaviors of 3-D frames can be numerically analyzed. Series of beam-column tests under varying axial load and unidirectional or bi-directional horizontal loads are performed, too. The comparison of the results of test and analysis proves sufficient accuracy of the analysis model.

A frame model considering the effects of varying axial loads is analyzed both under the static loads and under the dynamic earthquake loads. The results show that the neglect of the varying axial load on columns may sometimes lead to risky overestimate of the total frame resistance.

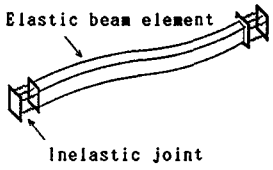

Fig.1 Beam-column Model

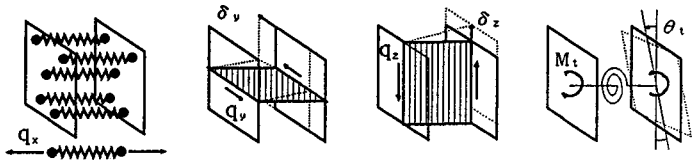

Fig.2 Elements of Multi-spring Inelastic Joint

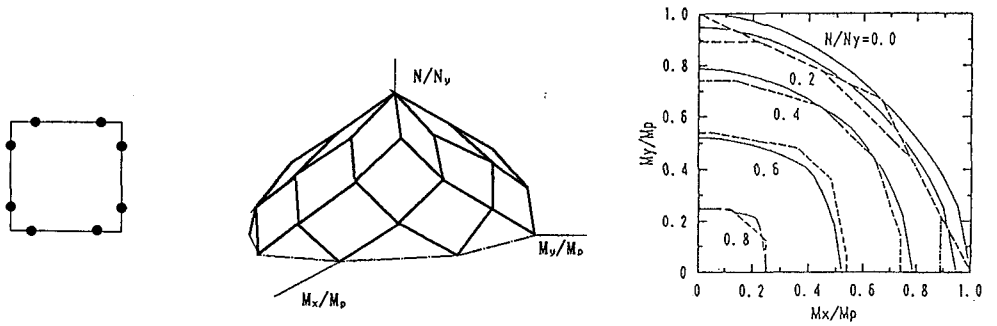

(a) Location of axial springs

(b) Relation between axial load and moments (in elastic perfectly plastic material)

(c) Projection of N-Mx-My relation on Mx-My plain
Real line: Box section
Dot line: Multi-spring model

Fig.3 Relation of resistance capacities of box sectional component

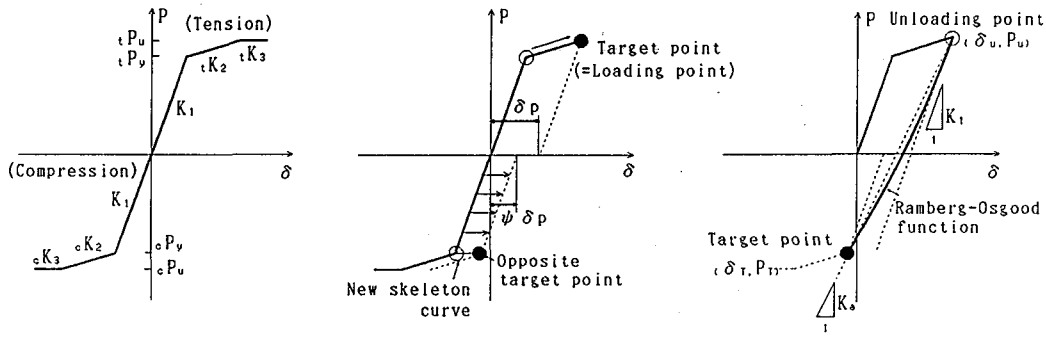

(a) Skeleton curves

(b) Shift of skeleton curves

(c) Unloading and reloading

Fig.4 Hysteresis Rule Used for Axial Spring

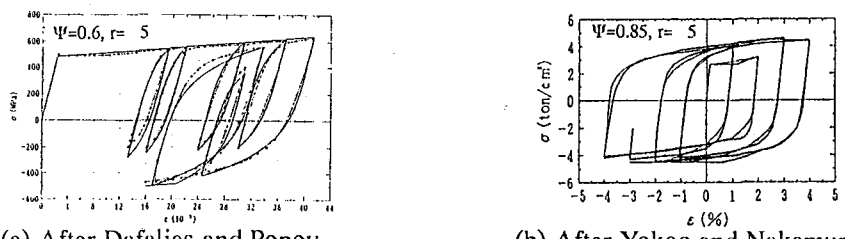

(a) After Dafalias and Popov

(b) After Yokoo and Nakamura

Fig. 5 Examples of Hysteresis Parameter Fitting

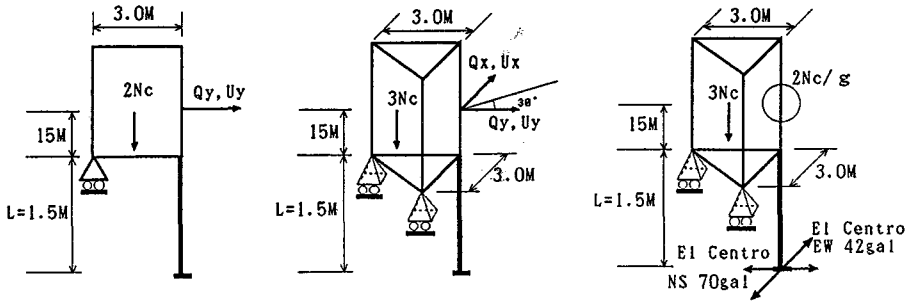

(a) Static loading test (unidirectional)

(b) Static loading test (bidirectional)

(c) Pseudo-dynamic test (bidirectional)

Fig.6 Fictitious Structural System Presumed in Loading Tests

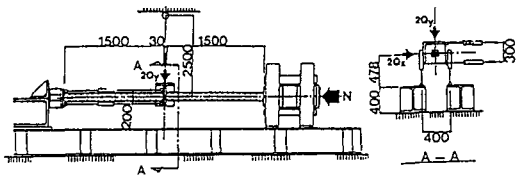

Fig.7 Test Rig

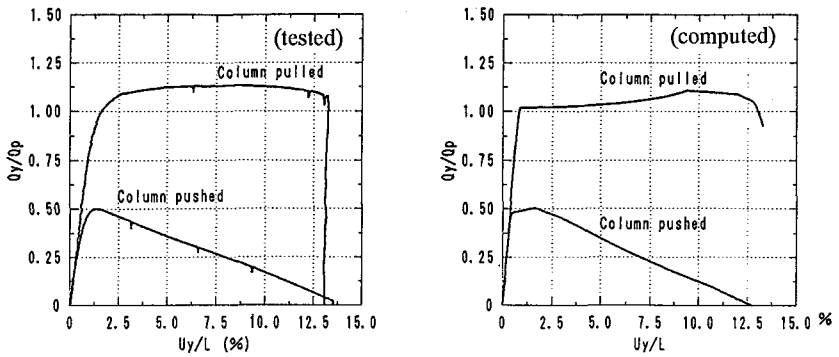

Fig.8 Results of Unidirectional Monotonic Loading Tests and Analysis

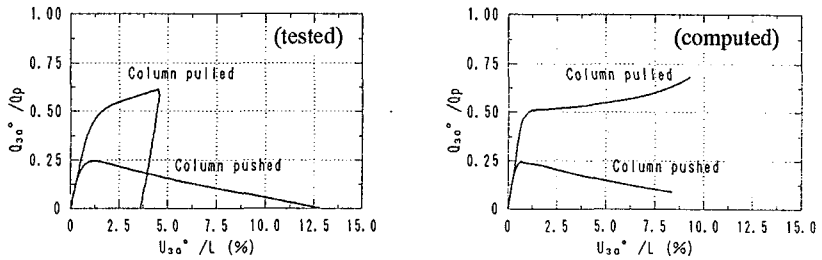

Fig.9 Results of Bidirectional Monotonic Loading Tests and Analysis

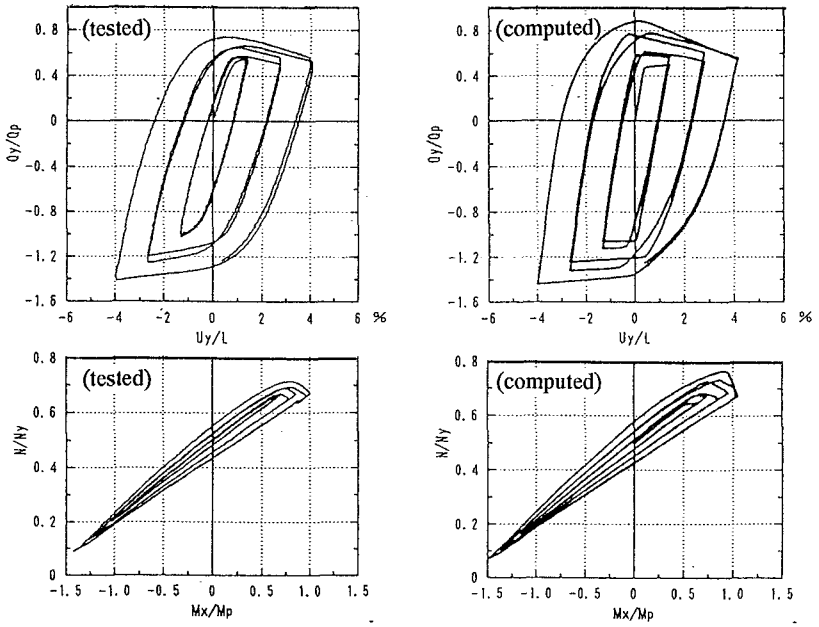

Fig.10 Results of Unidirectional Cyclic Loading Test and Analysis

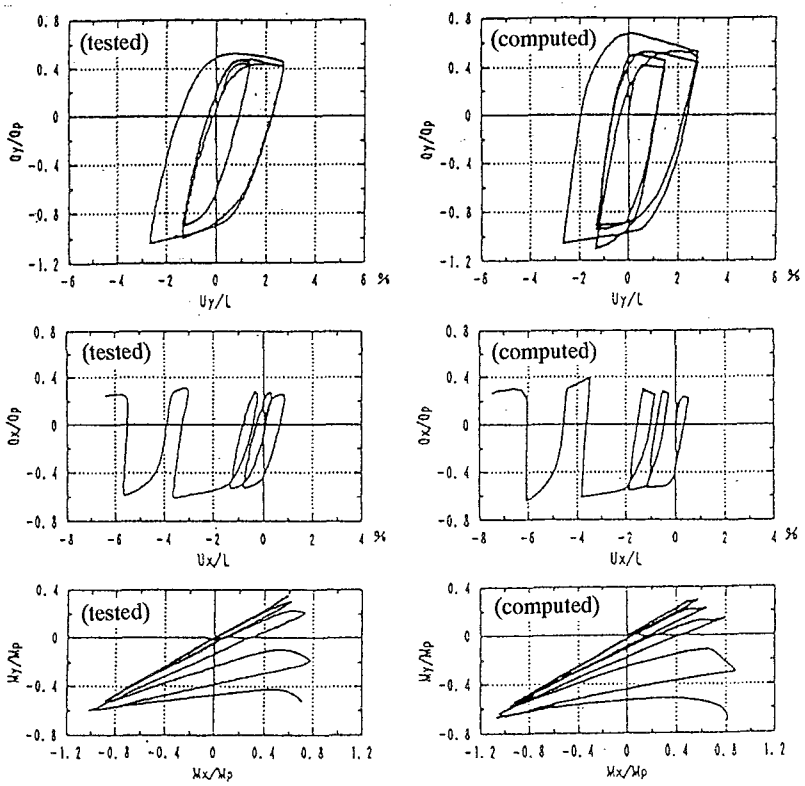

Fig.11 Results of Bidirectional Cyclic Loading Test and Analysis

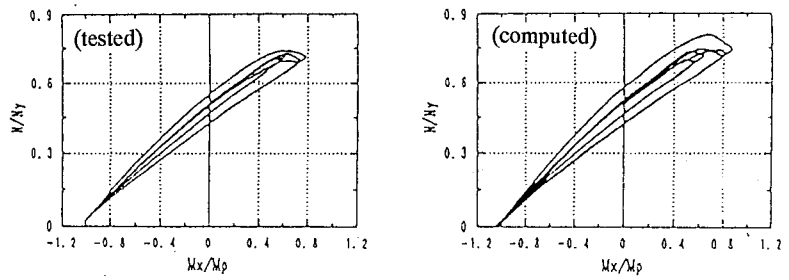

Fig.11 Results of Bidirectional Cyclic Loading Test and Analysis

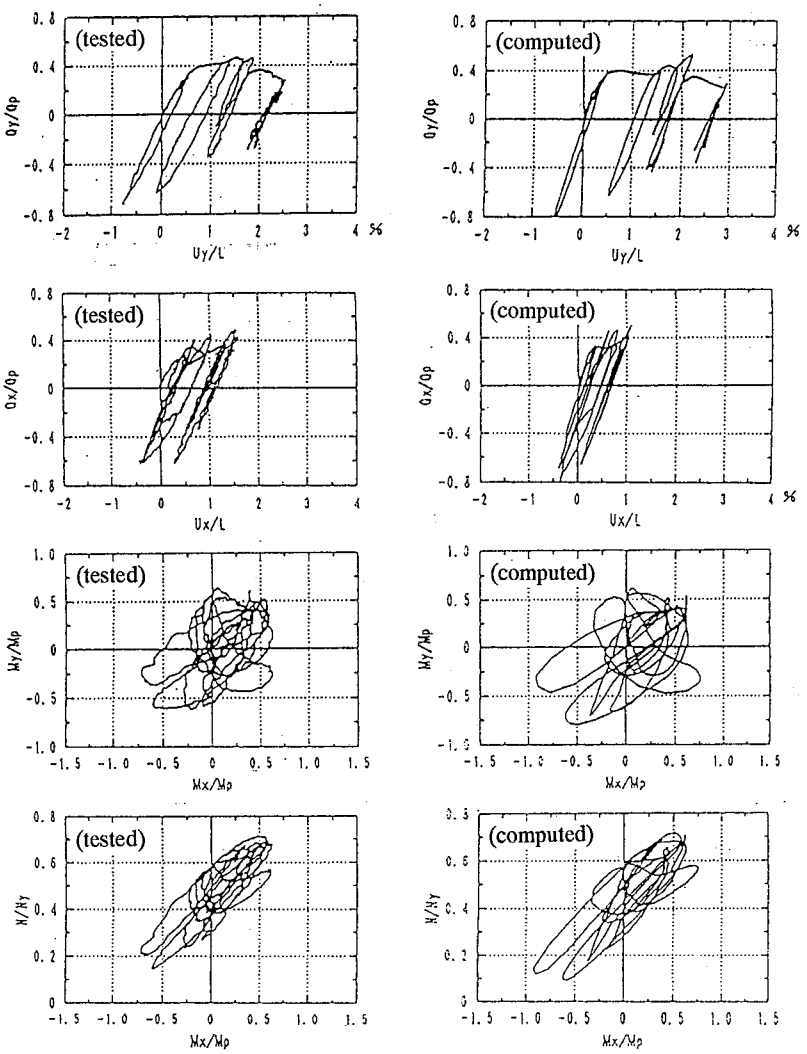

Fig.12 Results of Pseudo-dynamic Test under Bidirectional Earthquake Motion

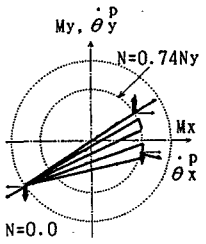

Fig.13 Cumulation of Plastic Rotation to One Side

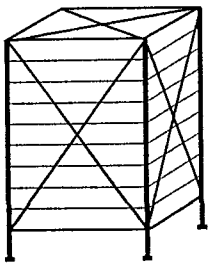

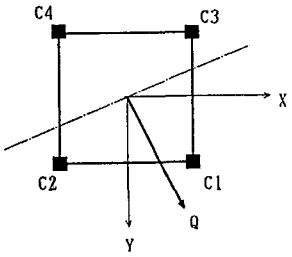

Fig.14 Analysis Frame Model

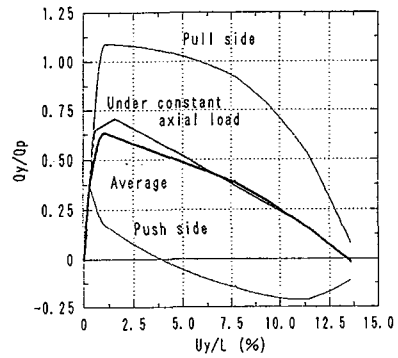

Fig.15 Results of Frame Analysis under Unidirectional Monotonic Load

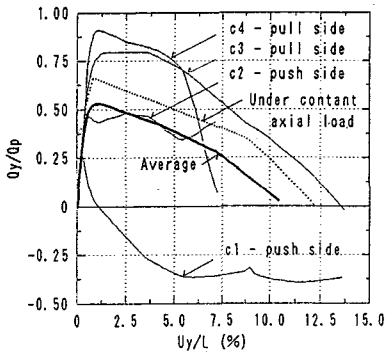

(a) Resistance vs. displacement along Y-axis

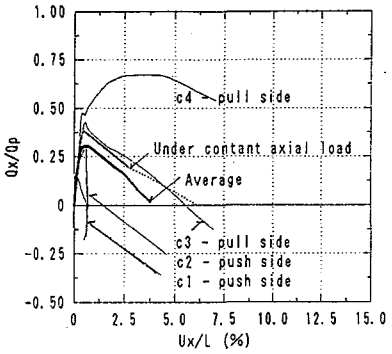

(b) Resistance vs. displacement along X-axis

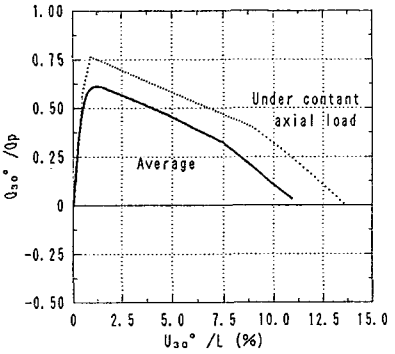

(c) Resultant resistance vs. displacement in the loading direction

Fig.16 Results of Frame Analysis under Bidirectional Monotonic Load

Acknowledgments

The authors gratefully acknowledge the financial support of the Ministry of Education, Science and Culture, Japanese Government, Grant in Aid for Scientific Research, No.0242208, No.04452243, which made this work possible. Also, the authors would like to express their appreciation to Mr.Y.Shimawaki and Mr. H.Kondo, Technical Officers of Institute of Industrial Science, for their supports during the test.

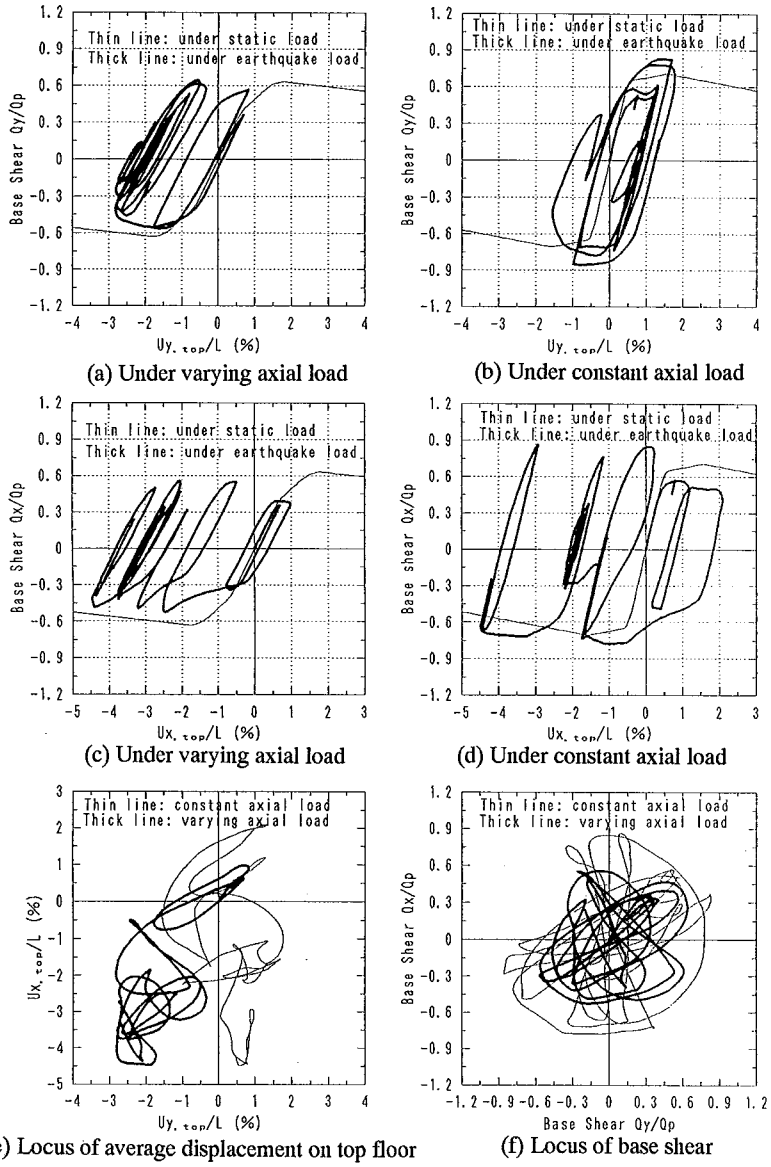

Fig.17 Results of Frame Analysis under Bidirectional Earthquake Motion

References

[1] K.Ohi, K.Takanashi, Y.Chen: "Intelligent Loading Tests on Steel Beam-columns under Varying Axial and Lateral Loads," ERS Bull.No.25, March 1992

[2] K.Ohi, K.Takanashi: "Multi-spring Model for Inelastic Behavior of Steel Members with Local Buckling," Stability and ductility of steel structures under cyclic loading, pp.215-224, CRC Press,1992

[3] Y.F.Dafalias, E.P.Popov: "Plastic Internal Variables Formalism of Cyclic Plasticity," Journal of Applied Mechanics, pp.645- 651, Dec. 1976

[4] Y.Yokoo, T.Nakamura, T.Komiyama: "Nonstationary Hysteretic Stress-Strain Relations of Wide-flange Steel and Moment-Curvature Relations under Presence of Axial Force," Pre. Rep., IABSE Symp., Lisboa,pp.143-149,1973